Ultra-Low-Noise, Single-Frequency, All-PM Thulium- and Holmium-Doped Fiber Amplifiers at 1950 nm and 2090 nm for Third-Generation Gravitational Wave Detectors

Patrick Baer, Pelin Cebeci, Melina Reiter, Florian Bontke, Martin Giesberts, and Hans-Dieter Hoffmann

***Abstract*—In the context of the E-TEST Interreg project, Fraunhofer ILT develops high stability, narrow linewidth laser seed sources and amplifiers at a wavelength of approx. 2 μm for potential usage in a third-generation gravitational wave detector: the Einstein telescope. While for such an application, there are highest demands on laser parameters such as linewidth, spectral purity, and polarization, especially stability properties such as the relative intensity noise must be optimized. To achieve highest output power stabilities, we develop a multi-stage low-noise holmium-doped fiber amplifier at a wavelength of 2095 nm, which is core-pumped by low-noise thulium-doped fiber lasers at a wavelength of approx. 1950 nm. In this article, we present the concept of the full laser system, and the achieved results for the pre-amplifier section, which perfectly fulfills the E-TEST pre-amplifier requirements. Our pump source, a thulium-doped fiber amplifier, achieves approx. 2 W output power at a wavelength of 1950 nm with 5 MHz linewidth and a polarization extinction ratio of 28 dB. With our holmium-doped fiber amplifier, we demonstrate an output power of approx. 400 mW at a wavelength of approx. 2095 nm with a linewidth of 2 MHz and a polarization extinction ratio of 18 dB. For both currently free-running systems we analyze the relative intensity noise (RIN) and obtained for example RINs of approx. 10^{-6} Hz$^{-0.5}$ at a frequency of 100 Hz, which shows the suitability of the concept to achieve highest stabilities. To evaluate our system, we perform a system performance analysis, where we present the influence of signal and pump wavelength, and signal and pump power on the achievable optical-optical efficiencies.**

***Index Terms*—Holmium-doped fiber laser, thulium-doped fiber laser, ultra-high stability, ultra-low-noise, single-frequency, relative intensity noise, gravitational wave detector.**

I. Introduction

GRAVITATIONAL wave detectors (GWD), such as Advanced LIGO, Advanced VIRGO and KAGRA, enable a new method for the exploration of the universe. The constant upgrades of the detectors and the resulting improvements of the measurement accuracy resulted in the very first direct detection of a gravitational wave in 2015 [1]. Until 2021, there are more than 90 candidates for detected events such as merging binary black hole and neutron star systems. Not only since the very first gravitational wave detection, next-generation gravitational wave detectors are pushed forward to further improve the measurement accuracies and achieve a higher detection rate.

In the context of the Interreg project E-TEST (Einstein Telescope EMR Site & Technology) [2], [3], a consortium consisting of several partners in Belgium, Germany and The Netherlands was founded, to demonstrate the feasibility and implementation of the Einstein Telescope in the Euregio Meuse-Rhine (EMR). Besides e.g., an underground study, several technologies such as a large, suspended silicon mirror at cryogenic temperatures or the required optical technologies for a laser interferometer shall be demonstrated and validated.

Since the to-be-used silicon mirrors are opaque at the typical GWD wavelength of 1064 nm, a longer laser wavelength for example in the range of 1500 nm to 2100 nm is required [4]. In comparison to a laser wavelength of 1550 nm, a wavelength around 2000 nm can for example be beneficial due to a lower optical absorption in amorphous silicon coatings [5], and to finally achieve the required measurement resolution [4]. In the E-TEST project, the consortium decided to focus on a wavelength of approx. 2090 nm and develop necessary optical technologies such as optimized photodiodes and coatings for this wavelength. Therefore, Fraunhofer ILT develops a laser system at a wavelength of approx. 2090 nm.

To fulfill the requirements, we decided to develop a seed laser based on a Ho:YAG crystals to define the spectral properties, and a multi-stage holmium-doped fiber amplifier for the amplification. The full E-TEST system will be presented in detail in Section II, in this article we will focus on the pre-amplifier section. While for usage in a gravitational wave detector there are highest requirements on typical laser parameters such as linewidth, spectral purity, and polarization, especially the stability properties such as the relative intensity noise (RIN) must be considered and optimized. To achieve the highly ambitious power stability properties, we decided to not only setup as stable as possible holmium-doped fiber amplifiers, but also as stable as possible pump lasers, namely thulium-doped fiber laser at

Manuscript received 26 September 2023; revised 22 December 2023; accepted 10 January 2024. Date of publication 16 January 2024; date of current version 13 February 2024. The work was supported in part by Interreg EMR, European Regional Development Fund (EFRE), and in part by the Ministry for Economic Affairs, Innovation, Digitalization and Energy of the State of North Rhine-Westphalia. *(Corresponding author: Patrick Baer.)*

The authors are with the Fraunhofer ILT-Institute for Laser Technology, 52074 Aachen, Germany (e-mail: patrick.baer@ilt.fraunhofer.de).

Digital Object Identifier 10.1109/JPHOT.2024.3354454

wavelengths of approx. 1950 nm, which are used for core-pumping of the holmium-doped fiber amplifiers. The long-term goal, defined in agreement with the ETpathfinder research facility, is to develop a 2090 nm laser system with approx. 1 kHz linewidth, linear polarization, a relative intensity noise $<10^{-6}$ $Hz^{-0.5}$ at 100 Hz, and a frequency noise <100 $Hz/Hz^{0.5}$ at 100 Hz at an output power of more than 10 W.

The state of the art in the development of single-frequency high stability lasers for GWD is highly dependent on the required wavelengths. At 1064 nm, fully functional and stabilized laser systems with >150 W output power have been successfully demonstrated for terrestrial GWD [6]. Several approaches for further power scaling are being evaluated [7], [8]. For the third generation of GWD, several other approaches are currently being pursued. For the space-based gravitational wave detector LISA, compact systems with an output power of approx. 2 W at a wavelength of 1064 nm are under development [9], [10]. For wavelengths at approx. 1550 nm and 1990 nm, systems are developed based on erbium-doped fibers [11] and thulium-doped fibers [12], respectively. To achieve wavelengths >2 μm, holmium-doped fibers can be a satisfactory solution. Using these holmium-doped fibers in fiber amplifier systems, average powers in the range of <10 W have been demonstrated [13], [14], [15]. However, to the best of our knowledge, for low-linewidth system based on holmium-doped fibers there are currently no publications on the relative intensity noise available, which is one of the most important requirements for a gravitational wave detector's laser.

In this article, we will present the results of the E-TEST pre-amplifier, which in its currently free-running configuration perfectly fulfills the E-TEST pre-amplifier requirements. In addition, this is to the best of our knowledge the first publication which analysis the frequency dependent relative intensity noise of a holmium-doped fiber amplifier. In the following section, we will first present our E-TEST laser concept, which is the long-term goal of the E-TEST project, consisting of the seed laser, the dual-stage holmium-doped fiber amplifier, and the corresponding pump lasers, based on thulium-doped fibers. In Sections III and IV, we will focus on the first amplifier stage, the holmium-doped fiber amplifier Ho1, and its pump laser, the first thulium-doped fiber amplifier Tm1. To start with, we will present the results of the thulium-doped fiber amplifier Tm1: the achieved output power, spectral properties, polarization, and especially the measured relative intensity noise properties. Afterwards, the holmium-doped fiber pre-amplifier concept and the corresponding results are presented with a focus on the achieved relative intensity noise for the currently free running, not actively stabilized system. For both presented systems, we achieve highest stabilities, especially at frequencies >100 Hz. In the end, we will give an outlook on our next steps, which are mainly focused on the further setup of the other laser stages and the active stabilization of the output signals. Overall, the presented system fulfills the E-TEST pre-amplifier requirements, and both presented thulium-doped and holmium-doped fiber amplifiers achieve highest power stabilities in their free-running configuration, which shows the suitability of the concept to achieve highest stabilities. In Section V we will present our detailed system performance analysis, where we performed a detailed system performance analysis. We showed the influence of four input parameters, namely the pump and signal power, and the pump and signal wavelength to show potential approaches for future holmium-doped fiber amplifier systems.

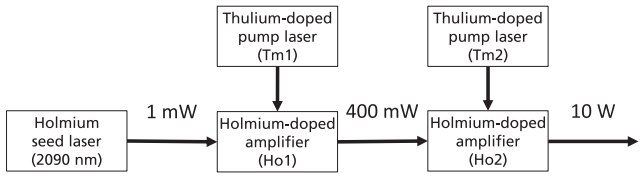

Fig. 1. Concept of the E-TEST laser system. In this article, the results of the pre-amplifier section will be presented, namely the thulium-doped pump laser Tm1 and the holmium-doped amplifier Ho1.

II. The E-TEST-Laser Concept

Fig. 1 shows the full laser concept we are developing in the context of the E-TEST project. It consists of a seeder, two holmium-doped fiber amplifier stages, and the corresponding pump sources. In the following, all stages will be presented.

The seed laser will be based on a Ho:YAG crystal to generate a wavelength of approx. 2090 nm. While we start with the development of a ring oscillator, the goal is to develop an NPRO-Seeder (Non-Planar Ring Oscillator) to achieve the low linewidth of approx. 1 kHz and fulfill the stability criteria in relative intensity noise and frequency noise. The seeder's pump laser will either be a Tm:YLF crystal based laser or a thulium-doped fiber laser.

To suppress nonlinear effects such as stimulated Brillouin scattering, to meet the required relative intensity noise parameters, and to reduce amplified spontaneous emission, the fiber amplifier itself is a two-stage holmium-doped fiber amplifier. The first stage (Ho1) is designed to amplify low power seed lasers with powers such as 1 mW to approx. 400 mW. In the second stage (Ho2), the power will be further amplified to approx. 10 W. It should be noted that both fiber amplifier stages and the corresponding pump sources are fully monolithic for an increased long-term stability and a more compact setup.

To achieve the highly ambitious power stability properties, we do not only setup as stable as possible holmium-doped fiber amplifiers, but also put a lot of effort into setting up as stable as possible pump lasers. The holmium-doped fiber amplifiers at 2090 nm are pumped by thulium-doped fiber lasers at a wavelength of approx. 1950 nm with low RIN. This way, we aim to achieve low pump laser noise which shall result in an overall lower noise in the holmium-doped fiber amplifier. In addition, the quantum defect in the holmium-doped fiber amplifiers shall be minimized, which can result in a high efficiency and an overall higher stability. The thulium-doped fiber lasers are either an amplifier (Tm1) and a resonator (Tm2). An advantage of our multi-stage laser design is that it reduces the dependence on the output power of the seed laser. Depending on the used seed source, only one or both fiber amplifier stages can be used. Therefore, the concept is highly adaptable, and our fiber amplifier system can be used to amplify alternative seed laser concepts, such as low linewidth fiber lasers or VECSEL.

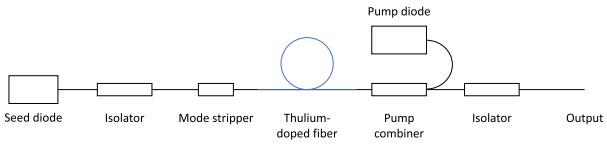

Fig. 2. Concept of the E-TEST thulium-doped pump laser Tm1 for amplification at a wavelength of approx. 1950 nm.

Another important aspect of our concept is that we have multiple active actuators that can potentially be used to control the output characteristics of the entire system. This includes for example the current and temperature of the used pump diodes. By actively regulating these parameters and implementing advanced stabilization mechanisms, for example the relative intensity noise could be improved. For monitoring of each of the single stages output characteristics, we implemented photodiodes in each single laser stage shown in Fig. 1, which can be an important tool for the active stabilization. We plan to use a similar method as we already used for studies of the European Space Agency ESA for future space-based gravitational-wave detectors, e.g., for LISA [16].

In the following, we will present the results of our currently non-stabilized, free running holmium-doped fiber amplifier Ho1, which is the pre-amplifier of the full E-Test laser system, and the corresponding pump laser the thulium-doped pump laser Tm1. The results presented are an important milestone towards the full laser concept shown in Fig. 1 and provide a suitable platform for later active power stabilization.

III. Experimental Results of the Thulium-Doped Fiber Amplifier Tm1

In the following, we present our results on the monolithic thulium-doped fiber amplifier (Tm1) as shown in Fig. 1, which is the pump laser for the holmium-doped fiber amplifier Ho1. The concept of the laser is shown in Fig. 2. As the seed source we use a fiber-coupled single-mode diode laser module at a wavelength of 1950 nm with a linewidth of approx. 5 MHz. It is amplified in a polarization maintaining thulium-doped fiber (iXblue, IXF-2CF-Tm-PM-10-130), which is contra-directionally pumped using fiber-coupled multi-mode diode laser modules with a wavelength of approx. 790 nm. For monitoring, we use several tap combiners and photodiodes which are not shown here. To protect the fiber amplifier from backscattered light and to filter unwanted amplified spontaneous emission from the amplifier, we use a fiber coupled isolator with a built-in bandpass filter at the end of the amplifier stage.

In Fig. 3 the output power with respect to the pump power is shown. Above the laser threshold, we measure an amplification with a slope efficiency of approx. 40% with respect to the pump power of the diode laser modules. By amplifying the approx. 10 mW output power of the seed diode, approx. we achieve approx. 2 W output power after the fiber coupled isolator. In Fig. 4, the measurement of the polarisation is shown, where we use a half-wave plate and a thin film polarizer. At full output power, we measured linearly polarized radiation with a

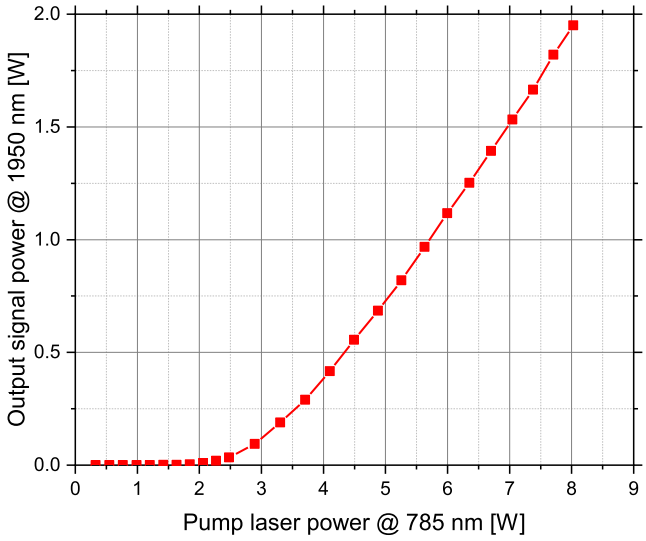

Fig. 3. Output power with respect to the pump power of the thulium-doped fiber amplifier Tm1.

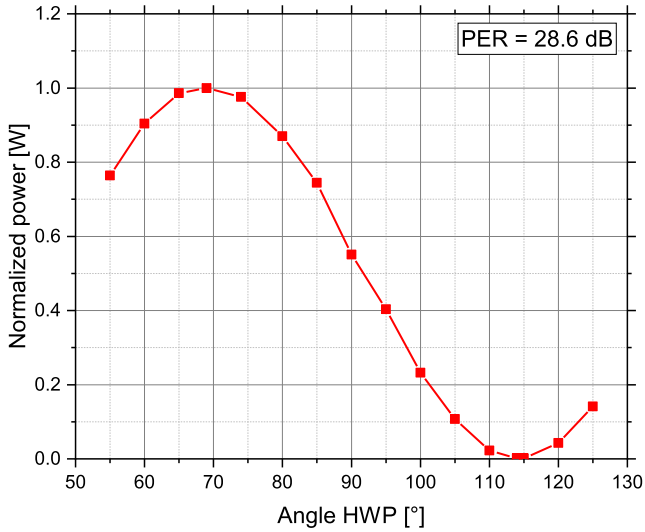

Fig. 4. Normalized power with respect to the half-wave plate angle of the thulium-doped fiber amplifier Tm1.

polarization extinction ratio of approx. 28.6 dB at the output of the fiber amplifier Tm1.

In Fig. 5 the normalized power with respect to the wavelength is shown for different power levels. The centre wavelength is at approx. 1953 nm. The measured linewidth of signal is wider than the specified 5 MHz, since our optical spectrum analyzer's resolution with 100 pm is too low. At a level of approx. -50 dB radiation can be measured from approx. 1945 nm to 1957 nm. We assume that this is no amplified spontaneous emission, but the amplified signal of the used seed lasers side modes. Based on the manufactureres data, the side-mode suppression ratio is approx. 45 dB, which is in good accordance to our measurements. In addition, the qualitative behaviour does not change with respect to the power level.

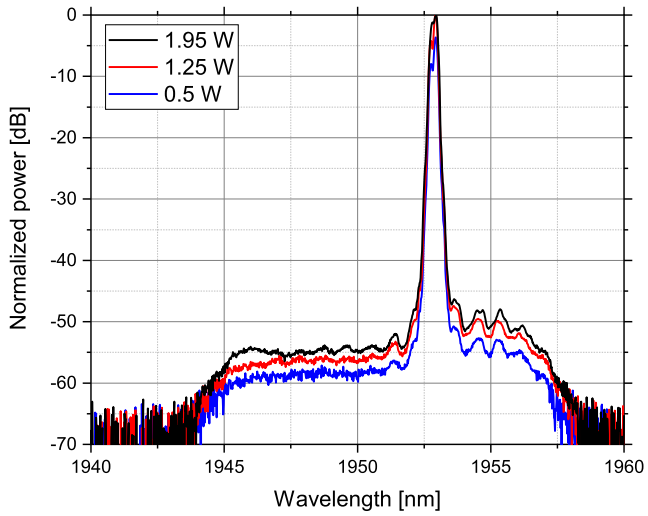

Fig. 5. Normalized power with respect to the wavelength of the thulium-doped fiber amplifier Tm1.

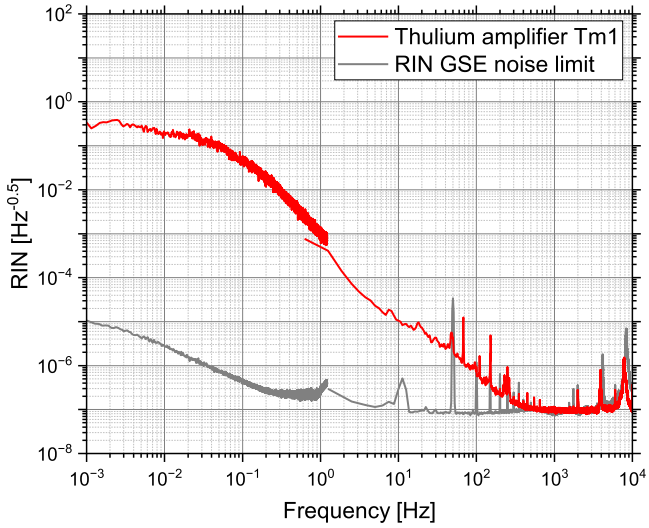

Fig. 6. Relative intensity noise of the thulium-doped amplifier Tm1 at full power operation and the GSE used for the measurement with respect to the frequency.

To analyze the temporal behaviour of the thulium-doped fiber amplifier's output power, we analyze the RIN using an in-house developed RIN-measurement setup. By doing this, we can identify the influence of noise sources at specific frequencies on the temporal stability of the laser's output power. With our current setup, we analyze frequencies from approx. 10^{-3} Hz to 10^{4} Hz. The RIN of the currently free-running thulium-doped amplifier Tm1 and RIN GSE (Ground Support Equipment) noise limit with respect to the frequency are shown in Fig. 6. At frequencies <1 Hz, we measure RINs of approx. $3{\cdot}10^{-1}$ $Hz^{-0.5}$ to 10^{-3} $Hz^{-0.5}$. This behaviour is expected, since our setup is currently not thermally stabilized and thermal effects play a crucial role in this frequency range. In the frequency range from 1 Hz to 500 Hz, we measure an approximately linear dependency of the RIN with respect to the frequency in this

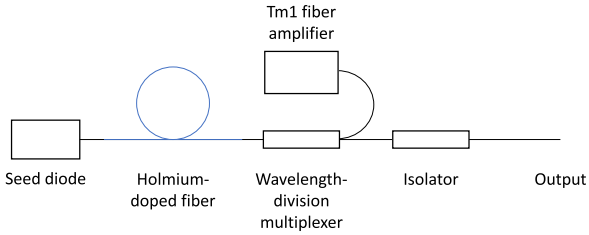

Fig. 7. Concept of the E-TEST holmium-doped fiber amplifier Ho1.

double logarithmic representation. Exemplary at 100 Hz, we achieve a RIN of approx. 10^{-6} $Hz^{-0.5}$. For frequencies >500 Hz, we are currently limited by the RIN GSE noise at a RIN level of approx. 10^{-6} $Hz^{-0.5}$ to 10^{-7} $Hz^{-0.5}$. Especially at high frequencies, we achieve satisfying results for the RIN. We expect that the RIN at lower frequencies of our currently free-running system can be improved by applying a thermal stabilization, to suppress thermal effects due to the lab environment.

IV. Experimental Results of the Holmium-Doped Fiber Amplifier Ho1

In this section, we present our results of the monolithic holmium-doped fiber amplifier (Ho1) as shown in Fig. 1. Fig. 7 shows the laser concept. Since the Ho:YAG seeder is still in development, we use a fiber coupled single-mode diode laser module with an output power of approx. 2 mW at a wavelength of approx. 2095 nm with a linewidth of approx. 2 MHz as a seed source. At low linewidth, stimulated Brillouin scattering (SBS) can be a power limiting nonlinear effect, which must be carefully considered in the fiber amplifier design. Currently, the seed laser's linewidth is still higher than the targeted 1 kHz linewidth. This can potentially result in a higher SBS threshold, since the SBS threshold is dependent on the linewidth. However, since the used laser linewidth is already well below the typical SBS bandwidth, we do not expect a significantly higher influence of SBS at lower linewidth. Therefore, our currently used seed laser can be used to demonstrate all the relevant fiber amplifier parameters.

The seed laser's radiation is amplified in a polarization maintaining holmium-doped fiber (iXblue, IXF-HDF-PM-8-125), which is contra-directionally pumped by the 1950 nm radiation emitted by the Tm1 pump laser presented in Section III by using a wavelength division multiplexer (WDM). As for the thulium-doped fiber amplifier Tm1, here we also use several tap combiners for monitoring of the signal, and a fiber coupled isolator with a built-in bandpass filter to protect the fiber amplifier from backscattered light and to filter unwanted amplified spontaneous emission.

In Fig. 8 the output power at 2095 nm with respect to the pump power at 1950 nm is shown. We achieve an output power of approx. 400 mW after the isolator, which has a transmission of approx. 68%. The achieved output power is perfectly fulfilling the E-TEST project goals and can be used as the input power for the Ho2 stage. However, based on our holmium-doped fiber simulation, we expected a higher slope efficiency. Therefore,

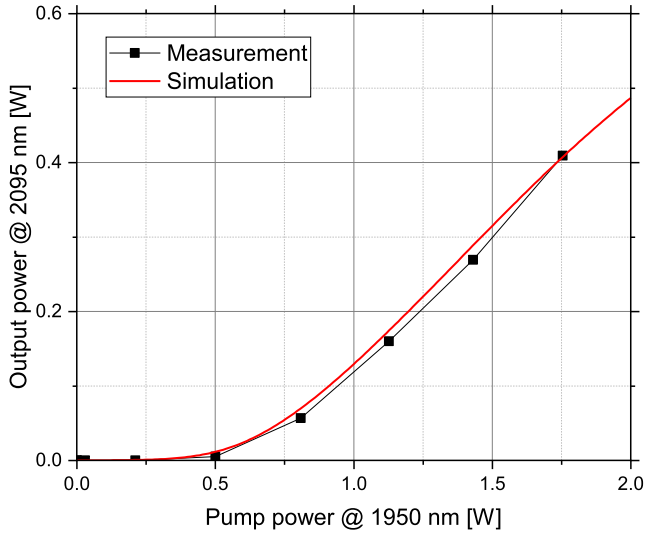

Fig. 8. Output power with respect to the pump power and simulation with adapter PIQ concentration of the holmium-doped fiber amplifier Ho1.

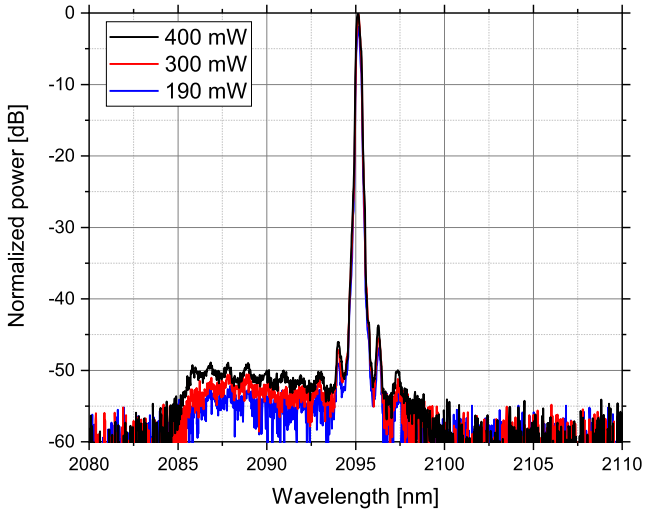

Fig. 10. Normalized power with respect to the wavelength of the holmium-doped fiber amplifier Ho1.

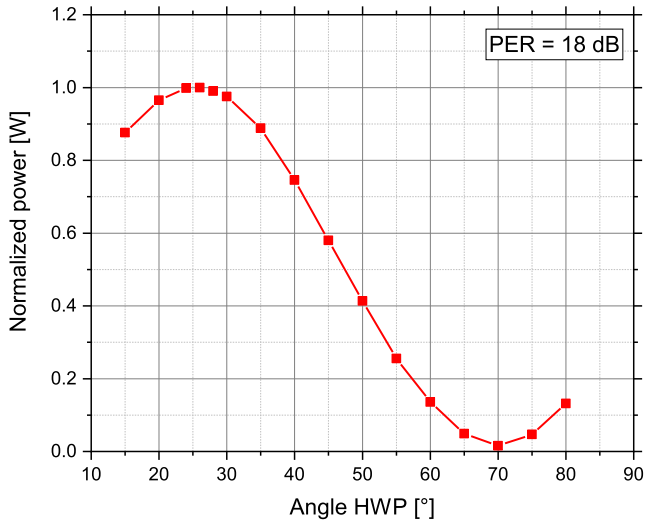

Fig. 9. Normalized power with respect to the half-wave plate angle of the holmium-doped fiber amplifier Ho1.

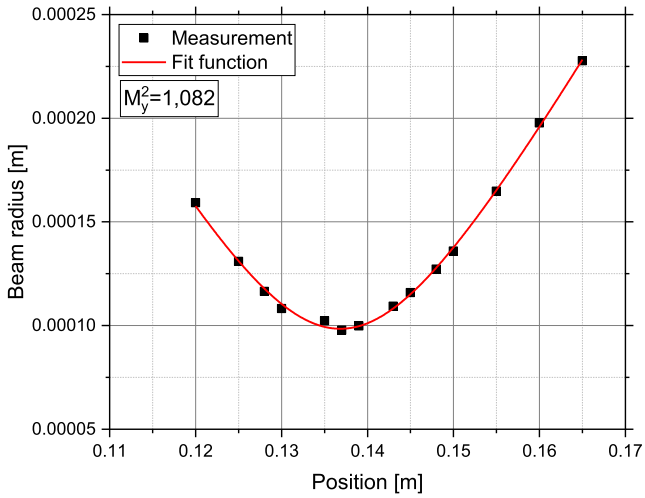

Fig. 11. Beam radius with respect to the lateral position in the beams optical axis of the holmium-doped fiber amplifier Ho1.

we performed additional tests to get information on the fiber's parameters, especially the pair-induced-quenching (PIQ). Using the cut-back method, we measured the small-signal absorption and the non-saturable absorption of the used fiber, and calculated the number of holmium ions 2k similar to other publications [17], [18]. Following this, we calculated that the number of holmium ions 2k within a cluster is approx. 6.9% for our used fiber, which results in a good agreement between the experimental results and our simulation as shown in Fig. 8.

In Fig. 9 the results of the polarisation measurement is shown. For this measurement, we use a half-wave plate and a thin film polarizer, resulting at full power operation in linear polarized radiation with a polarization extinction ratio of approx. 18. In Fig. 10 the normalized power with respect to the wavelength is shown for different power levels. The centre wavelength is at approx. 2095 nm, which corresponds to the seed laser wavelength. Similar to the 1950 nm laser, the measured signal linewidth is wider than the specified 2 MHz, because the resolution of our optical spectrum analyzer is too low. Besides the main peak at a wavelength of approx. 2095 nm, additional peaks with a periodicity of approx. 1 nm can be observed at power levels smaller than 45 dB. Since the periodity does not change for higher power levels, we expect that this is no ASE of the fiber amplifier, but the side modes of the seed diode. In addition, the manufactureres data sheets show a side-mode suppression ratio of 45 dB, which is in high agreement to our results.

In Fig. 11 the beam radius with respect to the position is shown. We obtain a beam quality factor M^2 of 1.082, which corresponds to a single-mode beam quality. All of these here parameters are perfectly in-line with the project goals for the

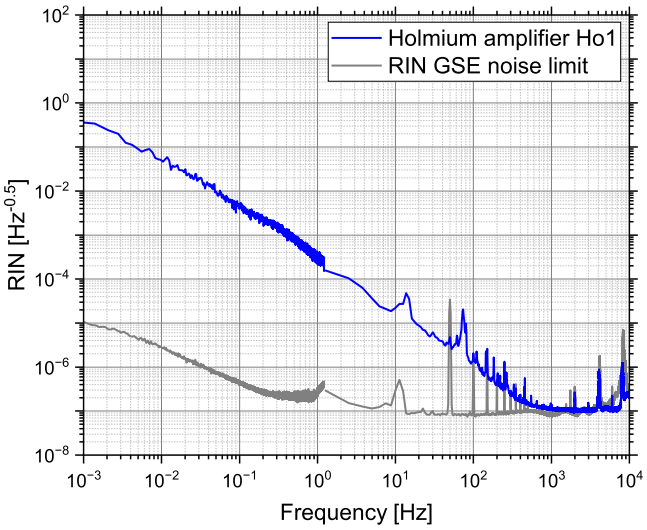

Fig. 12. Relative intensity noise of the holmium-doped fiber amplifier Ho1 at full power operation and the GSE used for the measurement with respect to the frequency.

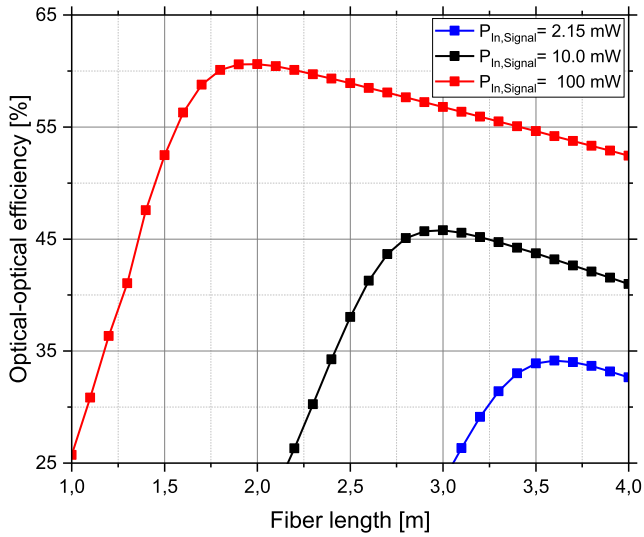

Fig. 13. Optical-optical efficiency with respect to the fiber length for an injected seed power of 2.15 mW, 10 mW and 100 mW.

Ho1 amplifier development and are an important step towards the demonstration of the parameters of the Ho2 amplifier stage.

To analyze the temporal behaviour of the holmium-doped fiber amplifier's output power, we analyze the relative intensity noise (RIN), as described in Section III. The RIN of the currently free-running, non-stabilized holmium-doped amplifier Ho1 and the RIN GSE noise limit with respect to the frequency are shown in Fig. 12. Overall, we measure similar results to the thulium-doped fiber amplifier Tm1, shown in Fig. 6. At frequencies $<$1 Hz, we measure RINs of approx. $3{\cdot}10^{-1}$ Hz$^{-0.5}$ to $2{\cdot}10^{-4}$ Hz$^{-0.5}$. Here we expect such a high RIN in comparison to the other frequencies, since our setup is currently not thermally stabilized and thermal effects play a crucial role in this frequency range. However, we measured a slightly better RIN at frequencies from 10^{-3} Hz to 1 Hz for the Ho1 amplifier stage than for the Tm1 amplifier stage. In the frequency range from 1 Hz to 1 kHz, we measure an approximately linear dependency of the RIN with respect to the frequency in the presented double logarithmic representation. At frequencies $>$1 kHz, we are currently limited by the RIN GSE noise. Here, we achieve RINs of approx. 10^{-6} Hz$^{-0.5}$ to 10^{-7} Hz$^{-0.5}$. Again, especially at frequencies $>$100 Hz, we achieve the most satisfying results. We expect that we can further improve the RIN at lower frequencies by applying a thermal stabilization, to reduce the influence of the lab environment onto the fiber amplifiers, and by applying an active power stabilization. Overall, the results show the suitability of the concept to achieve highest stabilities, currently especially at the high frequencies $>$100 Hz.

V. System Performance Analysis

As described in Section II, holmium-doped fiber amplifiers at 2090 nm can have a very low quantum defect when being pumped at 1950 nm. With our current system without usage of the final isolator, we achieve an optical-optical efficiency of approx. 34% as presented in Section IV. Even though the achieved relative intensity noise properties were the main goal of our fiber amplifier development, a higher overall optical-optical efficiency can be beneficial for further laser development. To analyze this, in the following section we will present a detailed theoretical analysis based on our numerical holmium-doped fiber amplifier simulation describing the influence of four E-TEST laser systems input parameters which are seed power, seed wavelength, pump power and pump wavelength on the overall optical-optical efficiency. We will present that our current system with its current design restrictions is very close to the theoretically possible efficiency value of 34.15%, being predicted by our holmium-doped fiber amplifier simulation.

In our analysis we study the influence of the parameters named above on the optical-optical efficiency, which we define as

$$\eta_{\mathrm{Opt}} = \frac{P_{\mathrm{Out,Signal}} - P_{\mathrm{In,Signal}}}{P_{\mathrm{Pump}}} \tag{1}$$

with the input and the output power of the signal, $P_{\mathrm{In,Signal}}$ and $P_{\mathrm{Out,Signal}}$, and the pump power P_{Pump}. In the whole analysis we will use the parameters of the holmium-doped fiber used to setup our holmium-doped fiber amplifier described in Section IV. By varying one of the fiber amplifier input parameters in the simulation, such as the pump wavelength, the optimal fiber length might change, which furthermore might influence the achievable optical-optical efficiency. Therefore, when varying a parameter, we will also identify the optimal fiber length, which we define as the length with the maximum optical-optical efficiency. While we only consider the optical-optical efficiency in our following analysis, we expect the slope efficiency to be higher than the optical-optical efficiency since the laser threshold is not considered in it. For high pump power, we expect the difference to be negligible.

Fig. 13 shows the optical-optical efficiency with respect to the fiber length for a signal input power of 2.15 mW, 10 mW

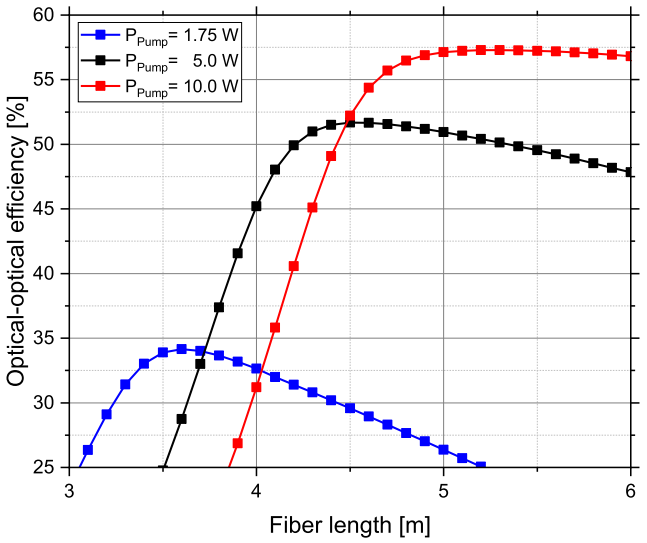

Fig. 14. Optical-optical efficiency with respect to the fiber length for an injected pump power of 1.75 W, 5.0 W and 10.0 W.

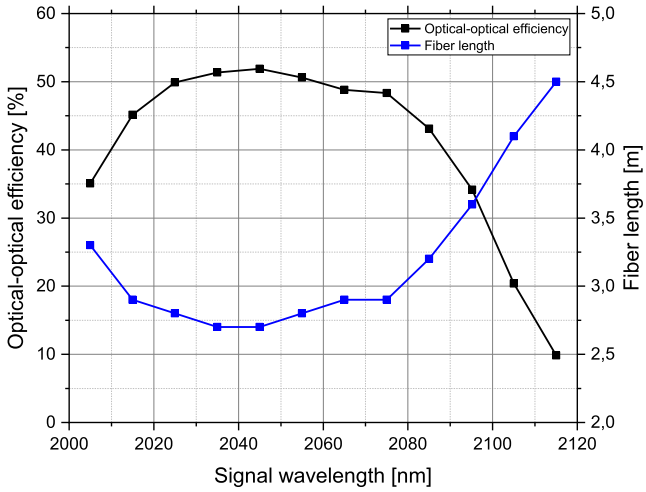

Fig. 15. Optical-optical efficiency and fiber length with respect to the signal wavelength.

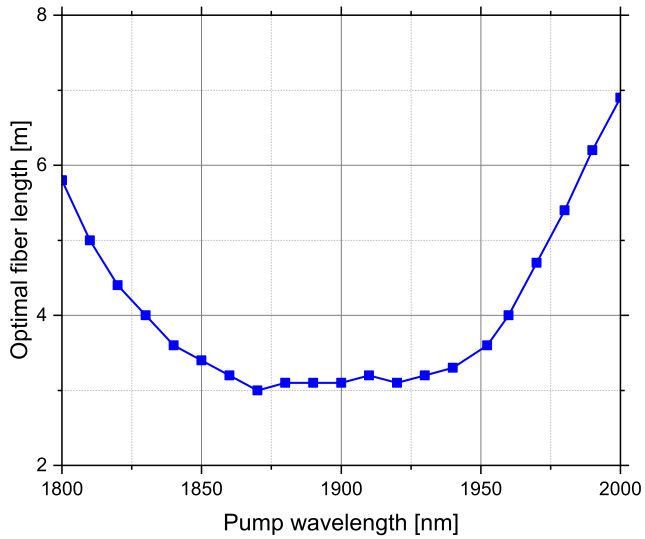

Fig. 16. Optimal fiber length with respect to the pump wavelength.

and for 100 mW at a signal wavelength of 2095.18 nm. For all three seed powers, the achievable optical-optical efficiency is highly dependent on the fiber length. For a signal input power of 2.15 mW and with a pump power of approx. 1.75 W at a wavelength of 1952 nm, our analysis shows that a maximum optical-optical efficiency of 34.15% is achievable, which is very close to our achieved optical-optical efficiency of 34%. For higher signal input powers, overall higher optical-optical efficiencies are achievable, such as approx. 45% for a signal input power of 10.0 mW and more than 60% for a signal input power of 100 mW. Overall, the seed power has a high influence on the achievable optical-optical efficiency.

In Fig. 14 the optical-optical efficiency with respect to the fiber length for an injected pump power of 1.75 W, 5.0 W and 10.0 W is shown. The pump wavelength is 1952.33 nm, while the seed signal has a wavelength of 2095.18 nm and a power level of 2.151 mW. As already shown for the signal power, the optical-optical efficiency increases for higher pump power levels. While for a pump power of 1.75 W an efficiency of approx. 34% is achievable, for 5 W and 10 W of pump power optical-optical efficiencies of approx. 51% and 57% are achievable, respectively. To absorb the higher amounts of pump power, longer fiber lengths are required.

In addition, we analyze the influence of the signal wavelength on the achievable optical-optical efficiency and the optimal fiber length. As described before, in context of the E-TEST project the consortium focused on a wavelength of approx. 2095 nm. However, changing the laser wavelength might be interesting for other applications. Fig. 15 shows the optimal fiber length and the corresponding optical-optical efficiency with respect to the signal wavelength. For a pump power of 1.75 W at a wavelength of 1952 nm and a signal power of 2.15 mW, the maximum optical-optical efficiency can be achieved at a wavelength of 2045 nm and reads 51.9%, which is approx. 17 percentage points higher in comparison to the achieved results of the E-TEST holmium-doped fiber amplifier. For higher signal wavelengths, even above the E-TEST laser wavelength, our simulation shows a lower efficiency.

To finalize our analysis, we analyze the performance of the holmium-doped fiber amplifier with respect to the pump wavelength. Due to the wavelength dependent cross-sections, we expect a high influence on the optimal fiber length. Therefore, we calculate, as already done before, the optimal fiber length for each pump wavelength, while keeping the other input parameters, the pump power of 1.75 W, the signal power of 2.15 mW and the signal wavelength of 2095.18 nm constant.

Fig. 16 shows the optimal fiber length with respect to the pump wavelength. From 1860 nm to 1940 nm, the optimal fiber length is approximately the same. For shorter and longer pump wavelengths, the optimal fiber length becomes longer in both cases.

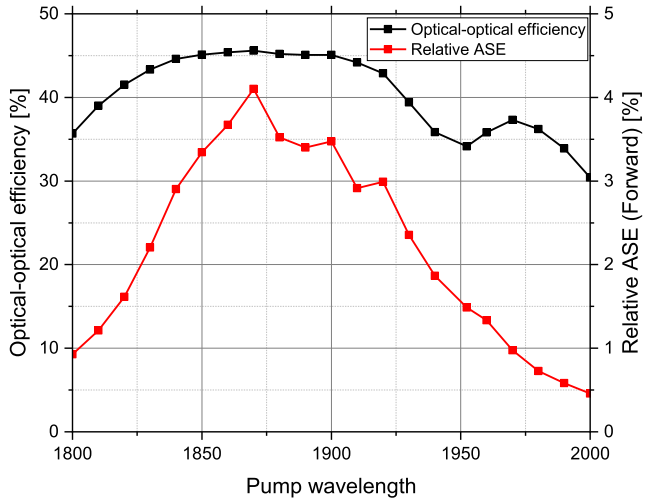

Fig. 17. Optical-optical efficiency and relative amplified spontaneous emission (ASE) in forward direction with respect to the pump wavelength.

In Fig. 17 the optical-optical efficiency and the relative amplified spontaneous emission (ASE) in forward direction with respect to the pump wavelength is shown. The relative ASE used in our analysis is defined using

$$h_{\mathrm{ASE}} = \frac{P_{\mathrm{ASE}}}{P_{\mathrm{Out,Signal}}} \tag{2}$$

and describes the power of the ASE in forward direction P_{ASE} with respect to the signal output power. Our simulation shows that for pump wavelengths ranging from 1840 nm to 1910 nm the highest optical-optical efficiencies of approx. 45% can be achieved. For shorter wavelengths, the optical-optical efficiency decreases. A local minimum is observable at a pump wavelength of approx. 1950 nm and a local maximum can be observed at 1970 nm. The optical-optical efficiency decreases for higher wavelengths. For the relative ASE, the global maximum can be observed at a wavelength of 1870 nm. Therefore, especially pump wavelengths which result in high optical-optical efficiencies, result in the highest amounts of relative ASE. For shorter and longer pump wavelengths, the relative ASE decreases. For example, at a pump wavelength of 1970 nm, where in our exemplary case an optical-optical efficiency of 37% is achieved, the relative ASE amounts to 1%, which could be a good trade-off between optical-optical efficiency and ASE power for future laser systems.

Overall, higher seed and pump power are beneficial for higher optical-optical efficiencies, while there is also a high influence on pump and signal wavelength. The highest optical-optical efficiencies with respect to the pump wavelength can be achieved for pump wavelengths around 1870 nm, however, the amplified spontaneous emission also has its maximum at these pump wavelengths. Dependent on the application of the laser system it must be evaluated whether a higher optical-optical efficiency is beneficial even though there is potentially a higher amount of amplified spontaneous emission.

VI. Conclusion

In this article, we presented the results of the E-TEST pre-amplifier, which in its currently free-running configuration perfectly fulfills the E-TEST pre-amplifier requirements. In addition, this is to the best of our knowledge the first publication which analyzes the frequency dependent relative intensity noise of a holmium-doped fiber amplifier. The laser system is developed for future usage in a third-generation gravitational wave detector, the Einstein telescope. While for such an application, there are highest demands on laser parameters such as linewidth, spectral purity, and polarization, especially stability properties such as the relative intensity noise must be optimized.

We presented the first holmium-doped fiber amplifier (Ho1) and its pump laser the thulium-doped pump laser (Tm1), which represent the first amplifier stage and its pump laser of the E-TEST laser concept. By not only developing an as stable as possible holmium-doped fiber amplifier, but also an as stable as possible thulium-doped fiber amplifier, which is used as the pump laser, we aim to fulfill the highly ambitious power stability properties. For Tm1, we achieve approx. 2 W output power at a wavelength of app. 1950 nm with 5 MHz linewidth, and linearly polarized output power with no signs of ASE. The relative intensity noise measurements show satisfying results, especially at high frequencies $>$100 Hz. For Ho1, we demonstrated an output power of approx. 400 mW at a wavelength of approx. 2095 nm with 2 MHz linewidth, a polarization extinction ratio of 18 dB and no amplifier-related ASE. We performed and analyzed the relative intensity noise of the fiber amplifier and achieve satisfying results especially at high frequencies, showing the suitability of the approach to achieve highest stabilities. For both currently free-running system, we achieved RINs of approx. 10^{-6} Hz$^{-0.5}$ at a frequency of 100 Hz. The results presented are perfectly fitting to the E-TEST project goals of the first amplifier stage and are an important milestone towards the full laser concept, and our thulium- and holmium-doped fiber amplifier provide a suitable platform for later active power stabilization. To further analyze the optical-optical efficiency of our system, we performed a detailed system performance analysis. Here, we showed the influence of four input parameters, namely the pump and signal power, and the pump and signal wavelength. Overall, higher seed and pump power are beneficial for higher optical-optical efficiencies, while there is also a high influence on pump and signal wavelength. The highest optical-optical efficiencies with respect to the pump wavelength can be achieved for pump wavelengths around 1870 nm, however, the amplified spontaneous emission also has its maximum at these pump wavelengths. Based on our analysis, especially a pump wavelength at 1970 nm could be a good trade-off between optical-optical efficiency and the amount of ASE power.

Our next steps are the setup of the further stages Tm2 and Ho2 for higher power amplification of the achieved 400 mW to $>$10 W. In addition, we plan to further test the here presented amplifier system with a seed laser with smaller linewidth. Furthermore, we are preparing thermal stabilization and active power stabilization tests to further improve the relative intensity noise, especially at the low frequencies.

REFERENCES

[1] B. P. Abbott et al., "Observation of gravitational waves from a binary black hole merger," *Phys. Rev. Lett.*, vol. 116, no. 6, 2016, Art. no. 61102, doi: 10.1103/PhysRevLett.116.061102.

[2] E-TEST Einstein Telescope Emr Site & Technology, 2023. [Online]. Available: https://www.etest-emr.eu/

[3] A. Sider et al., "E-TEST prototype design report," 2022, *arXiv:2212.10083*.

[4] R. X. Adhikari et al., "A cryogenic silicon interferometer for gravitational-wave detection," *Classical Quantum Gravity*, vol. 37, no. 16, 2020, Art. no. 165003, doi: 10.1088/1361-6382/ab9143.

[5] J. Steinlechner et al., "Silicon-based optical mirror coatings for ultrahigh precision metrology and sensing," *Phys. Rev. Lett.*, vol. 120, no. 26, 2018, Art. no. 263602, doi: 10.1103/PhysRevLett.120.263602.

[6] P. Kwee et al., "Stabilized high-power laser system for the gravitational wave detector advanced LIGO," *Opt. Exp.*, vol. 20, no. 10, pp. 10617–10634, 2012, doi: 10.1364/OE.20.010617.

[7] F. Wellmann et al., "Low-noise, single-frequency 200 W fiber amplifier," *Proc. SPIE*, vol. 11260, pp. 125–131, Feb. 2020. [Online]. Available: https://www.spiedigitallibrary.org/conference-proceedings-of-spie/11260/2543292/Low-noise-single-frequency-200-W-fiber-amplifier/10.1117/12.2543292.full

[8] P. Cebeci et al., "Highly stable, high power hybrid fiber and Innoslab amplifier for narrow linewidth signals," *Proc. SPIE*, vol. 11259, pp. 121–127, Feb. 2020. [Online]. Available: https://www.spiedigitallibrary.org/conference-proceedings-of-spie/11259/2545934/Highly-stable-high-power-hybrid-fiber-and-Innoslab-amplifier-for/10.1117/12.2545934.full

[9] J. B. Camp, M. A. Krainak, A. W. Yu, and K. Numata, "Laser system development for gravitational-wave interferometry in space," *Proc. SPIE*, vol. 10511, pp. 182–188, Jan./Feb. 2018. [Online]. Available: https://spiedigitallibrary.org/conference-proceedings-of-spie/10511/2289051/Laser-system-development-for-gravitational-wave-interferometry-in-space/10.1117/12.2289051.full

[10] P. Cebeci et al., "Highly stable fiber amplifier development and environmental component-testing for the space-based gravitational wave detector LISA," *Proc. SPIE*, vol. 12400, pp. 162–167, Jan./Feb. 2023. [Online]. Available: https://www.spiedigitallibrary.org/conference-proceedings-of-spie/12400/2649881/Highly-stable-fiber-amplifier-development-and-environmental-component-testing-for/10.1117/12.2649881.full

[11] F. Meylahn and B. Willke, "Characterization of laser systems at 1550 nm wavelength for future gravitational wave detectors," *Instruments*, vol. 6, no. 1, 2022, Art. no. 15, doi: 10.3390/instruments6010015.

[12] Q. Zhang et al., "5 W ultra-low-noise 2 μm single-frequency fiber laser for next-generation gravitational wave detectors," *Opt. Lett.*, vol. 45, no. 17, pp. 4911–4914, 2020, doi: 10.1364/OL.402617.

[13] R. E. Tench et al., "Two-stage performance of polarization-maintaining holmium-doped fiber amplifiers," *J. Lightw. Technol.*, vol. 37, no. 4, pp. 1434–1439, Feb. 2019, doi: 10.1109/JLT.2019.2894973.

[14] L. G. Holmen and H. Fonnum, "Holmium-doped fiber amplifier for pumping a $ZnGeP_2$ optical parametric oscillator," *Opt. Exp.*, vol. 29, no. 6, pp. 8477–8489, 2021, doi: 10.1364/OE.419939.

[15] P. Baer et al., "Thulium- and holmium-doped high stability fiber amplifiers at 2 μm for next generation gravitational wave detectors," *Proc. SPIE*, vol. 12400, pp. 54–57, Jan./Feb. 2023. [Online]. Available: https://www.spiedigitallibrary.org/conference-proceedings-of-spie/12400/2649611/Thulium--and-holmium-doped-high-stability-fiber-amplifiers-at/10.1117/12.2649611.full

[16] O. Fitzau et al., "Highly stable fiber lasers for satellite-based gravitational measurement," *Proc. SPIE*, vol. 10897, pp. 411–421, Feb. 2019. [Online]. Available: https://www.spiedigitallibrary.org/conference-proceedings-of-spie/10897/2509950/Highly-stable-fiber-lasers-for-satellite-based-gravitational-measurement/10.1117/12.2509950.full

[17] J. L. Gouët, F. Gustave, P. Bourdon, T. Robin, A. Laurent, and B. Cadier, "Realization and simulation of high-power holmium doped fiber lasers for long-range transmission," *Opt. Exp.*, vol. 28, no. 15, pp. 22307–22320, 2020, doi: 10.1364/OE.394011.

[18] P. Myslinski, D. Nguyen, and J. Chrostowski, "Effects of concentration on the performance of erbium-doped fiber amplifiers," *J. Lightw. Technol.*, vol. 15, no. 1, pp. 112–120, Jan. 1997, doi: 10.1109/50.552118.